

Transport and mineralization rates in North Sea sandy intertidal sediments, Sylt-Rømø Basin, Wadden Sea

*Dirk de Beer, Frank Wenzhöfer, Timothy G. Ferdelman, Susan E. Boehme, and Markus Huettel*¹
Max-Planck-Institute for Marine Microbiology, Celsiusstrasse 1, D-28359 Bremen, Germany

Justus E. E. van Beusekom

Alfred-Wegener-Institut for Polar and Marine Research/Wadden Sea Station Sylt, Hafenstrasse 43, D-25992 List/Sylt, Germany

Michael E. Böttcher, Niculina Musat, and Nicole Dubilier

Max-Planck-Institute for Marine Microbiology, Celsiusstrasse 1, D-28359 Bremen, Germany

Abstract

We investigated the rates of the main microbiological processes (primary production, aerobic and anaerobic carbon degradation) and transport phenomena in an intertidal sand plate with a combination of in situ microsensor measurements and incubations. The sand was coarse, organically poor (0.6–1 mg of total organic carbon per gram dry weight of sediment), and highly permeable to water flow ($k = 1.5\text{--}7 \times 10^{-11} \text{ m}^2$). Aerobic respiration rates ranged from 105 to 175 $\text{mmol m}^{-2} \text{ d}^{-1}$, sulfate reduction rates from 0.08 to 13.7 $\text{mmol m}^{-2} \text{ d}^{-1}$, and net primary production $<35 \text{ mmol m}^{-2} \text{ d}^{-1}$. In situ microsensor measurements showed large changes in oxygen and sulfide concentrations in the top 10 cm, depending on tides and waves. The observed dynamics and high aerobic degradation rates imply that pressure gradients drive advective influx of oxygen and organic material from the water column into the sediments. Our results show that intertidal porous sand plates have high aerobic degradation rates, despite having an organic matter content that is one to two orders of magnitude lower than that of fine-grained deposits with similar decomposition rates.

Sandy sediments are generally thought to harbor less microbial activity than muddy sediments because of the lower organic matter content and microbial cell numbers (Jickells and Rae 1997; Llobet-Brossa et al. 1998). The large grain size with relatively low specific surface area results in rather low adsorption capacity and, therefore, ostensibly low microbial activities (Keil et al. 1994; Jickells and Rae 1997). Thus, although sands cover ~70% of the coastal zones of the North Sea, most biogeochemical research has been directed to muddy areas. Our goal was to determine the major microbial activities of intertidal sand flats: the rates of benthic primary production and degradation of organic matter. The flux of organic material and electron acceptors from the overlying seawater and their transport within the sediment usually determine benthic degradation rates. In addition, benthic photosynthesis might be a significant source of organic matter and oxygen. In fine-grained silt and clay sediments, transport is to a large extent diffusional. In contrast, in the upper layers of coarse sediments, advection is the dominant transport process (Malcolm and Sivyer 1997). Wa-

ter movement in permeable sediments is driven by the hydrodynamics of the overlying waterbody (i.e., by currents over ripples; Forster et al. 1996) and by wave action (Rutgers Van Der Loeff 1981; Precht and Huettel 2003), as well as by burrowing macrofauna. Intertidal flats are exposed to tides, possibly inducing further enhancement of pore-water exchange (Rocha and Cabral 1998). In laboratory chamber experiments, it was demonstrated that advective pore-water flows affect oxygen penetration into the sediment (Booij et al. 1991). This was confirmed in flume experiments (Ziebis et al. 1996), revealing that oxygen penetration depth increased by a factor of 10 upstream of protruding sediment structures because of water intrusion into the bed. The advective transport is not restricted to solutes but also includes particles. Permeable sediments were shown to act as a filter for planktonic algae that were transported into the sediment with the interfacial water flows, thereby enhancing the organic matter flux to the sediment (Huettel and Rusch 2000; Rusch and Huettel 2000). The circulation of water through the pores of permeable sediment enhances the mineralization rate of dissolved and particulate organic matter, and such sediments therefore might play a more important role in the oceanic carbon cycle than is generally assumed (Shum and Sundby 1996). Both organic material and electron acceptor can be transported rapidly into porous sediments, so intertidal sands might be hot spots of aerobic and anaerobic degradation activity (Kerner 1993; Kerner and Yasserli 1997; D'Andrea et al. 2002).

Intertidal flats are exposed to a complex combination of variable environmental factors, such as tides, currents, air

¹ Present address: Florida State University, Oceanography, West Call Street OSB517, Tallahassee, Florida 32306-4320.

Acknowledgments

We thank Ursula Werner for an essential discussion and two reviewers for constructive comments. Gaby Eickert, Vera Hübner, and Anja Eggers are thanked for preparation of the microsensors; Stephan Meier and Volker Meyer for technical help; and the staff and workers of Hafenlabor (Alfred Wegener Institute, Sylt) for their hospitality.

exposure, storms, and different light intensities and temperature ranges. This greatly complicates assessment of the actual conversion rates in these sediments. Samples collected in the field and examined in the laboratory are no longer exposed to the in situ conditions; thus, transport rates of oxygen and organic material are different. Therefore, transport and conversion rates are best determined in situ. The highly dynamic nature of the environment and accessibility during the tidal cycles complicates in situ studies of intertidal areas. Typically, during interesting periods (i.e., during a storm), intertidal flats cannot be monitored (Jickells and Rae 1997). The equipment for in situ measurements will change the hydrodynamic regime and thus the exchange rate in permeable sediments. Because conversions in sediments are transport limited, it is unavoidable that the instrumentation will influence the measured rates. In situ exchange rates have been determined with benthic flux chambers (Huettel and Gust 1992; D'Andrea et al. 2002), but the area under investigation is physically isolated from its surroundings; thus, the hydrodynamics and transport phenomena are changed. Ideally, the equipment should be minimally invasive, weather-proof, and stand-alone, to allow measurements during bad weather.

In the search for a more open measuring system, we have deployed microsensors on an automatic measuring platform. Microsensors are minimally invasive because of their small size and thin shafts and are assumed to have only a small effect on local hydrodynamics. Microsensors were mounted on automatic profiling equipment to enable continuous measurements over periods of days. From microprofiles, measured in situ, exchange rates can be calculated (Archer et al. 1989; Glud et al. 1994a; Komada et al. 1998). However, in order to interpret microprofiles, accurate quantification of transport rates is necessary (Berg et al. 1998). In porous sands, both advection and diffusion play a role. Moreover, analyses should take place during steady-state conditions, which rarely occur in these dynamic environments. We have approached these problems by combining field and laboratory measurements. By a combination of microsensor techniques (in situ and on retrieved cores), as well as field studies with benthic chambers, we have determined consumption, production, and exchange rates of oxygen and compared them with sulfate reduction rates measured with radiotracers.

Materials and methods

Site description—The Wadden Sea is a coastal sea along the Dutch, German, and Danish North Sea coast. Most of the Wadden Sea is protected from the North Sea by barrier islands. The Wadden Sea is strongly influenced by tides. Diurnally, about 50% of the sediments in the Wadden Sea are exposed during low tide. These tidal flats consist mostly of sandy sediments and sediments of mixed grain size (Asmus et al. 1998). The investigated intertidal sand flat is part of the Sylt-Rømø Basin in the North Frisian Wadden Sea near the German-Danish border. The tidal amplitude is ~2 m. The islands Sylt and Rømø are connected to the mainland by a causeway. Therefore, the main water exchange occurs through the inlet to the North Sea. Freshwater input is of

minor importance. The field site is located directly south of the harbor in List on the island of Sylt and 300 m from the “harbor laboratory” of the Wadden Sea Sta. Sylt. It stretches along the coast over a distance of ~500 m, and the measurements were performed in the middle section. The site is protected from currents by a short dam and from the prevailing westerly winds by the island. At low tide, the flats are usually exposed, whereas at high tide, the water level is 1–2 m, depending on weather and tides. The origin of the sand is mainly eolic, blown in from the island. We present measurements from two sites, located ~100 m apart. The first site is at the midway line between the high and low waterline, ~40 m in the offshore direction from the high waterline. The second location is about 1 m in the land direction of the low waterline.

Microsensors, profiler—Microsensors for O₂ and H₂S were prepared as described previously (Jeroschewski et al. 1996; Reusbech 1989). To prevent damage from the coarse sand, the sensor tips were prepared with a thick wall, resulting in a tip diameter of ~300 μm, whereas the actual sensing surface was 5 μm. The response times (t_{90}) were <5 s. The sensors were calibrated after mounting on a deep-sea profiling lander, as described previously (Gundersen and Jørgensen 1990; Wenzhöfer et al. 2000; Wenzhöfer and Glud 2002). In addition to the solute microelectrodes, a resistivity microelectrode was mounted on the profiler to detect the sediment surface and to determine the ripple movements and heights. The profiler was preprogrammed to measure a series of vertical profiles, with a step size of 2,500 μm over a depth of 5–10 cm. For the photosynthesis measurements, a step size of 1,000 μm was chosen to a depth of 2 cm. Because each profile measurement took 20–30 min and was followed by a pause of 30 min, the temporal resolution was ~1 h. The profiler was placed on the intertidal flat during low tides and the sensors were positioned at ~1 cm from the surface at the start of the profiling. The profiling was continued for one or two tidal cycles, after which the data were downloaded for further processing and the profiler was serviced for the next deployment.

Occasionally, manual oxygen microsensor measurements were performed, in particular at the low waterline. The sensor was then mounted on a micromanipulator attached to a heavy stand. The readings were made directly from the display of the battery-powered amplifier, and positioning was accomplished by manually operating the micromanipulator. The manual measurements during incoming tide were possible up to a water depth of 35 cm.

Oxygen consumption rates—Sediment cores (3.5 cm diameter) were collected and immediately brought to the field station. The bottom stopper was fitted with a valve and tubing that was connected to a peristaltic pump so that water could be pumped from the bottom of the core, resulting in perfusion of the sand column, with rates from 0.01 to 4 ml min⁻¹. Freshly aerated seawater was continuously added to the water column above the sediment. An oxygen microsensor was positioned at a defined depth in the sediment. At the beginning of a measurement, seawater was pumped through the sediment in a downward direction, resulting in oxygen-

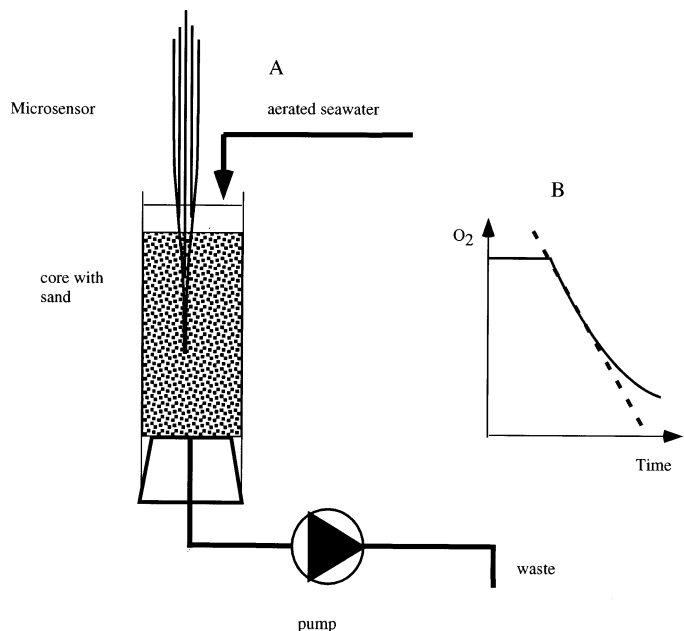


Fig. 1. (A) Equipment scheme for measuring the local respiration rate. A microsensor is positioned in a sediment core that is connected to a pump to allow downward flow. (B) A sketch of the procedure. When the oxygen concentration is constant, the downward perfusion is stopped, leading to an instant oxygen decrease (dotted line) that is equal to the respiration rate.

ation of the sediment. After steady state was reached, as determined by a constant oxygen concentration, the pump was switched off for about 1 min. The decrease in oxygen concentration was used to calculate the local oxygen uptake rate. The procedure was repeated at least three times at each depth, after which the sensor was repositioned to another depth for the next activity measurement. The setup and experiment is illustrated in Fig. 1.

Sulfate reduction rates—Potential sulfate reduction rates were determined with the whole-core $^{35}\text{SO}_4^{2-}$ injection method (Jørgensen 1978). Subcores were taken from the tidal flat during the flooding tide with 26-mm-diameter Plexiglas core tubes and transported at 4°C back to the Bremen radiochemical laboratory in less than 12 h. The subcores were injected at 1-cm intervals with $\sim 4 \mu\text{l}$ of $50 \text{ kBq } \mu\text{l}^{-1} \text{ }^{35}\text{SO}_4^{2-}$ (Amersham) contained in filtered North Sea water. Sediments were incubated at temperatures reflecting in situ conditions for 2–4 h. Because the radiotracer incubations were not performed immediately and in situ, the results must be considered potential rates of sulfate reduction. Bacterial activity was halted by slicing the cores at 1-cm intervals and placing the sediment slices into an equal volume of 20% (w/v) zinc acetate and freezing (-20°C). ^{35}S incorporation into total reducible inorganic sulfur was determined by the one-step acidic Cr-II method (Fossing and Jørgensen 1989).

During the October 1999 sampling excursion, zones of sediment near *Arenicola* spp. burrows were sampled selectively. Sediment (triplicate samples of $\sim 1 \text{ g}$) from *Arenicola* spp. burrow linings and from surrounding, nonburrow sediment was collected and stored cool in 3-ml glass vials (Ve-

noject) and stoppered. Sets of samples (burrow, nonburrow) were collected from the upper gray oxidized zone and from the black reduced sediment. In Bremen, the vials were degassed with N_2 , $400 \text{ kBq } ^{35}\text{SO}_4^{2-}$ tracer was added, and the samples were incubated for 2 h before terminating bacterial activity by freezing. Before Cr-II distillation, sediments were thawed in 20% (w/v) zinc acetate.

In addition to the standard whole-core technique, sulfate reduction rates also were measured on one sediment core used for measuring oxygen consumption rates (*see Oxygen Consumption Rates*) during the July 2000 sampling excursion. Rather than injecting tracer into the side of the core, 80 ml of seawater spiked with 2 MBq of $^{35}\text{SO}_4^{2-}$ (25 kBq ml^{-1} ; 890 MBq mol^{-1} sulfate) was perfused into the upper 10 cm of the core. The core was then incubated at near-in situ temperature (room temperature) for 2 h and sectioned at 4-mm intervals. The sediment was preserved and processed as described above.

Pore water extraction—Pore-water samples for the assessment of nutrient distributions in the sediment were collected with a pore-water sipper. Six profiles were measured in March and six in July 2000. The sipper had ports at 25, 50, 75, 100, 125, and 150 mm depth that were connected via gas-tight tubing to a multiple syringe sampler. The sampling device was described in detail previously (Huettel 1990). From each depth, a pore-water volume of 15 ml was extracted, and in addition, a water sample 1 cm above the sediment surface was taken with a separate syringe. All samples were passed through $0.2\text{-}\mu\text{m}$ filters without air contact to vacuum vials and preserved with HgCl_2 . Nutrients were determined with a Scalar[®] autoanalyzer (Grasshoff et al. 1999). Dissolved sulfate was quantified gravimetrically as BaSO_4 from pore water that was fixed in Zn acetate solution immediately after sectioning sediment cores into 1-cm slices at the field station (Llobet-Brossa et al. 2002).

Sediment properties—Porosity was determined from the weight loss on drying at 60°C for 72 h. To determine the carbonate content, the porosity samples were wetted and incubated in an HCl atmosphere for 48 h. Subsequently, the sediments were dried again at 60°C for 72 h. This treatment results in exchange of CO_3^{2-} by Cl^- , and the resulting dry-weight loss and the difference in molecular mass of Cl^- and CO_3^{2-} were used to calculate the carbonate content. Total organic carbon and total nitrogen were determined on freeze-dried sediment slices with an elemental analyzer (Carlo Erba EA1500). Sediment permeability profiles were measured on sections of freshly retrieved cores (3.6 cm diameter, 20 cm length) with a constant head permeameter (Klute and Dirksen 1986). Cores for solid-phase iron extraction were frozen (-20°C) until extraction. The fraction of iron extractable with a dithionite–citrate acetic acid solution (reactive Fe) was determined on dried sediments as described previously (Canfield 1989). Sediments were extracted under continuous agitation at room temperature for 1 h. Extracted iron was measured spectrophotometrically with the use of Ferrozine as described previously (Thamdrup et al. 1994), and the results were corrected for the contribution from iron monosulfide. Acid-volatile sulfur (AVS, essentially iron monosul-

fide) was determined on samples that had been preserved in Zn acetate solution in the field as part of the two-step Cr(II) distillation procedure (Fossing and Jørgensen 1989), in which the H_2S was trapped quantitatively as Ag_2S in a AgNO_3 solution and quantified gravimetrically.

Benthic chambers—The two benthic chambers deployed in March and July 2000 to assess oxygen fluxes with and without an advective transport component were made of acrylic cylinders (19 cm inner diameter, 33 cm height), covered with black foil to exclude light. The cylinders were pushed ~22 cm into the sediment, producing enclosed water volumes of 3,100–3,330 ml. The water in one cylinder was stirred by a disc (15 cm diameter) rotating at 24 rpm at 6.5 cm above the sediment, whereas the water column in the second cylinder was stagnant. This rotation generated a pressure gradient of 1.2–1.5 Pa between the center and rim of the chamber. This pressure gradient is similar to those generated by the interaction of the sediment ripples at the study site with a boundary flow of 10 cm s^{-1} at 10 cm above the sediment (Huettel and Gust 1992); thus, it should be considered a conservative setting. In permeable sediments, this pressure gradient causes advective pore-water exchange. Therefore, the stirred chamber could be used to assess the effect of advective pore-water exchange at a known pressure gradient. In the control chamber, the water column was not stirred, except briefly for 2 s before each sampling to ensure an equal distribution of solutes in the water column and to avoid the build up of a concentration gradient in the chamber. Initial injection of 2 mmol Na-bromide dissolved in 10 ml of seawater into the chambers permitted the assessment of advective exchange. At time intervals ranging between 1 and 3 h, three 10-ml water samples were taken from both chambers by glass ampoules and immediately analyzed for oxygen content by Winkler titration (Grasshoff et al. 1999). Additionally, three 2-ml samples were taken for bromide content measurement. The water volume removed was replaced with an equal volume of filtered seawater.

Organic carbon determination in the water column—During 2001, water samples were taken twice weekly at two nearby stations along the main channel of the Sylt-Rømø Basin. The sampling was carried out in the framework of a long-term monitoring program (Martens and Elbrächter 1998). For particulate organic carbon measurements, 100 ml of seawater was filtered through GF/C filters. The filters were stored at -20°C until analysis. C and N content were measured with an element analyzer after removing inorganic carbonate with HCl fumes (Grasshoff et al. 1999). Filtrate was stored frozen, and analyses for dissolved organic phosphorus followed the method of Grasshoff et al. (1999).

Ribosomal RNA analyses—Samples were taken in the middle of the flat ~40 m from the high waterline during low tide in October 1999, March 2000, and July 2000. The sediment cores were kept at in situ temperature during transport, subsampled within 2 h (sectioned in 1-cm layers), and stored at -80°C until further use. RNA was extracted from 2–8 ml of wet sediment (per layer) by bead beating, phenol extraction, and isopropanol precipitation as described previously

(Stahl et al. 1988; MacGregor et al. 1997). The quality and purity of RNA was checked with an Agilent 2100 Bioanalyzer (Agilent Technologies, Ambion).

Up to 50 ng of RNA was blotted onto nylon membranes (Magna Charge; Micron Separations) in triplicate and hybridized with ^{32}P radioactively labeled oligonucleotide probes as described previously (Stahl et al. 1988). The probes used were UNI 1390 (GACGGGCGGTGTGTA-CAA), which targets all known forms of life (Zheng et al. 1996), and EUB 338 (GCTGCCTCCCGTAGGAGT), which is specific for bacteria (Amann et al. 1990). Hybridization signal intensity was measured with a PhosphorImager (Molecular Dynamics) and quantified relative to reference RNA (*Escherichia coli* rRNA standard; purchased from Roche).

Results

Sand properties—The sediment is a coarse, silicate sand with a median grain size of 200–400 μm and a porosity of 35–45%. In March, permeability decreased from $7 \times 10^{-11} \text{ m}^2$ at 1.5 cm to $4.5 \times 10^{-11} \text{ m}^2$ at 5 cm and $1.5 \times 10^{-11} \text{ m}^2$ at 10 cm. In July, permeability decreased more rapidly with depth ($6 \times 10^{-11} \text{ m}^2$ at 1.5 cm, $2.5 \times 10^{-11} \text{ m}^2$ at 5 cm, and $1.5 \times 10^{-11} \text{ m}^2$ at 10 cm depth). However, all these values characterize a highly permeable sediment. The sediment contained only 10–20 mg $\text{CaCO}_3 \text{ g}^{-1}$ dry weight, and the total organic carbon was 0.6–1 mg g^{-1} dry weight. During two 12-h profiler deployments in July 2001, the ripple movement and height were determined with a resistivity electrode. Both deployments showed a ripple amplitude of ~5 mm. During the flooding period of the first deployment, ripples passed the measurement site approximately every 80–190 min.

Pore-water and sediment chemistry—The pore-water nutrient profiles in March and July (Fig. 2) reflected the effect of advective transport in the upper 5 cm of the sediment column and diffusion below. In March, the silicate, phosphate, ammonia, and nitrate concentrations in the upper 5 cm of the sediment were similar to those in the overlying water column, and below 5 cm, the profiles were more typical for reduced coastal sediments: silicate, phosphate, and ammonia increased as expected from the build-up of mineralization products, whereas nitrate sharply decreased because of denitrification. Ammonia profiles indicated a concentration maximum at 7.5 cm sediment depth, indicating higher bacterial mineralization activities at the boundary of oxidized and anoxic sediment domains. Below that depth, ammonia concentrations decreased again. In July, the effect of advective flushing of the upper sediment layer was not as obvious, which might be related to reduced boundary flow conditions and decreased sediment permeabilities because of enhanced microbial and algal activities.

The sulfate concentrations in the pore water were at all depths close to bottom-water values (data not shown).

Extractable Fe bound as Fe(III) oxyhydroxides and Fe(II) monosulfides was measured seasonally in a number of cores, and typical results are shown in Fig. 3. Ferric iron, presumably in the form of oxyhydroxides or Fe(III)OOH, dominated the pool of extractable sedimentary iron. Concentrations of Fe(III) in the upper 5 cm ranged between 1,900 and 2,700

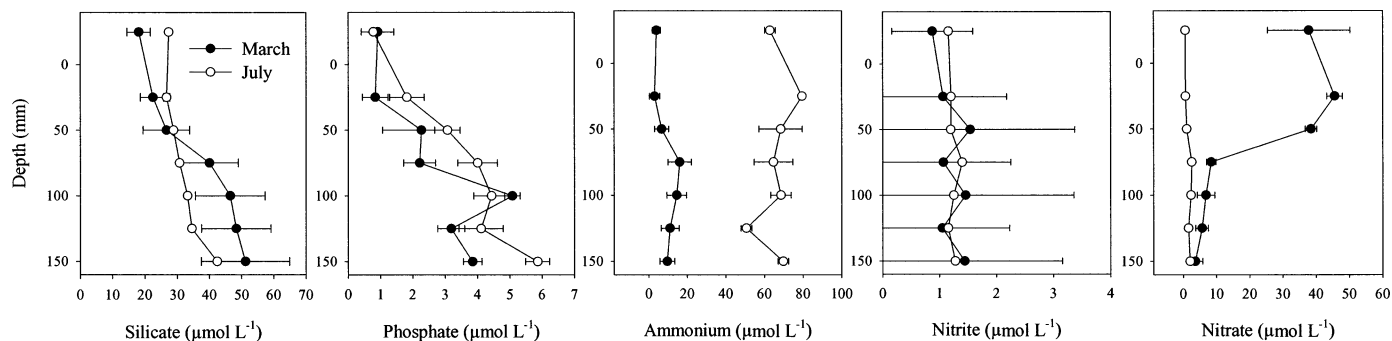


Fig. 2. Profiles of several compounds from pore water extracted in situ with a sipper during March and July 2000.

$\mu\text{mol Fe kg}^{-1}$ and exhibited no seasonal pattern. Below 5 cm depth, Fe(III) concentrations decreased with increasing depth, sometimes to $<1,000 \mu\text{mol Fe kg}^{-1}$. Decreases in Fe(III) concentration were often correlated with increases in Fe(II)S. Fe(II)S concentrations, in contrast to Fe(III), exhibited a high degree of seasonal and depth variability. Concentrations of Fe(II)S were near or below detection ($<4 \mu\text{mol Fe kg}^{-1}$) at the surface and then increased with increasing depth to concentrations of up to $1,000 \mu\text{mol Fe kg}^{-1}$ before decreasing again to low or nondetectable concentrations at greater depths. The peak in Fe(II)S varied seasonally from 10–13 cm depth in March 1999 to 3–9 cm during the warmer months.

O₂ fluxes measured in the benthic chambers—The in situ chamber incubations (Fig. 4) confirmed the results obtained from the nutrient profiles, with doubled oxygen consumption rates in the stirred chambers causing advective flow compared with the nonstirred chamber with diffusive and possibly limited biogenic oxygen transport into the sediment. The relatively regular oxygen concentration decreases in both chambers on both measuring days in July suggested

that larger bioirrigating macrofauna organisms were not present in the incubated sediments. The oxygen fluxes calculated for the stirred chambers (64 and $49 \text{ mmol m}^{-2} \text{ d}^{-1}$) and stagnant chambers (36 and $24 \text{ mmol m}^{-2} \text{ d}^{-1}$) were relatively high. The bromide tracer revealed that diffusive transport into the sediment corresponded to a fluid volume exchange of $5 \text{ L m}^{-2} \text{ d}^{-1}$, whereas advective exchange caused a tracer loss corresponding to $64 \text{ L m}^{-2} \text{ d}^{-1}$ in the stirred chamber. Thus, the oxygen uptake is increased by stirring-induced pore-water exchange.

In situ O₂ and sulfide dynamics—The O₂ and H₂S dynamics were investigated with microsensors at two sites on the intertidal sand flat. We first describe the observations near the low waterline, then those at the site midway between the high and low waterline. An overview of the field measurements reported in this paper is given in Table 1.

At the low waterline, only manual O₂ measurements were

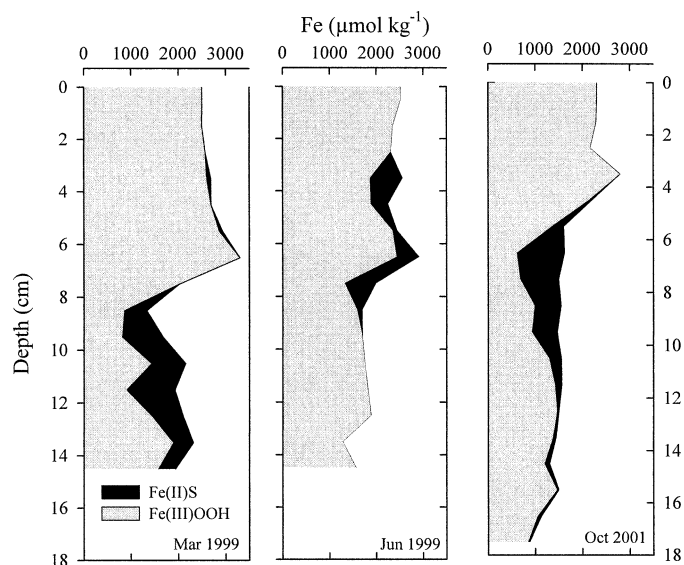


Fig. 3. Depth profiles of extractable “reactive” Fe(III) as shown by the gray-shaded area and Fe(II)S as shown by the black-shaded area for three of the sampling periods.

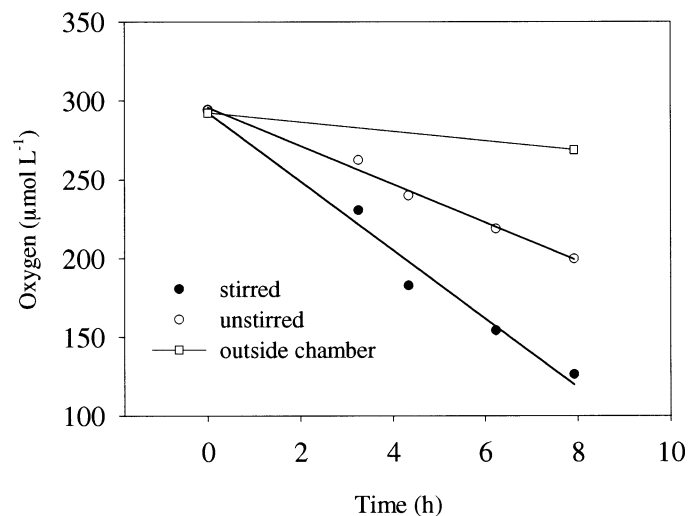


Fig. 4. Benthic oxygen concentration decrease in a stirred and unstirred benthic chamber deployed at the study site in July 2000. The chambers did not permit light penetration to the sediment. The oxygen concentrations outside the chamber were measured at the start and end of the incubation. The sediment respiration rate was stimulated by stirring at 24 rpm, generating a pressure gradient of 1.2–1.5 Pa between the center and rim of the chamber. Bromide was added to the chambers to assess advective exchange between sediment and enclosed water volume.

Table 1. Overview of the field measurements and summary of the results.

Sampling date	Measurements	Results
Mar 99	Manual O ₂ and H ₂ S measurements at low waterline Solid-phase Fe and S extractions	Fast penetration of O ₂ with incoming tide, no H ₂ S detectable Fe(II)S and Fe(III)OOH concentrations
Jun 99	Manual O and H ₂ S measurements on middle flat Whole-core ³⁵ SO ₄ ²⁻ experiments Solid-phase Fe and S extractions	Free H ₂ S present, all O ₂ sensors broken Potential sulfate reduction rates Fe(II)S and Fe(III)OOH concentrations
Oct 99	Automatic O ₂ and H ₂ S measurements at midway flat, manual at low waterline Whole-core ³⁵ SO ₄ ²⁻ experiments Ribosomal RNA analysis	O ₂ and H ₂ S dynamics during one tidal cycle, fast penetration of O ₂ with incoming tide Potential sulfate reduction rates Total and bacterial RNA content
Mar 00	Automatic O ₂ and H ₂ S measurements on midway flat Whole-core ³⁵ SO ₄ ²⁻ experiments Benthic chamber deployments Pore water extractions Sediment core sampling Ribosomal RNA analysis	O ₂ dynamics during several tidal cycles, no H ₂ S detectable Potential sulfate reduction rates Oxygen consumption rates Nutrient profiles Permeability and porosity data Total and bacterial RNA content
Jul 00	Automatic O ₂ and H ₂ S measurements on midway flat Whole-core and perfusion method ³⁵ SO ₄ ²⁻ experiments Benthic chamber deployments Pore-water extractions Sediment core sampling Ribosomal RNA analysis	O ₂ and H ₂ S dynamics during several tidal cycles Potential sulfate reduction rates Oxygen consumption rates Nutrient profiles Permeability and porosity data Total and bacterial RNA content
Nov 00	Manual O ₂ and H ₂ S measurements at low waterline	Rapid penetration of O ₂ with incoming tide, no H ₂ S detectable
Oct 01	Solid-phase Fe and S extractions	Fe(II)S and Fe(III)OOH concentrations

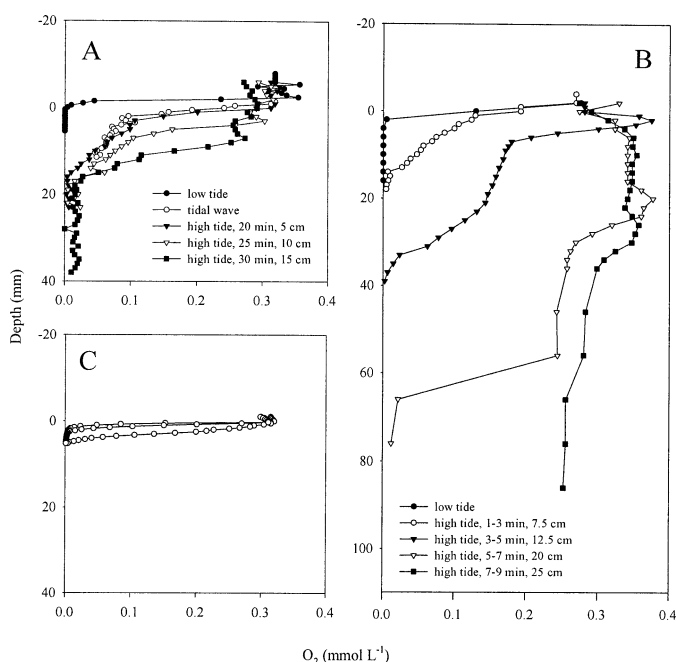


Fig. 5. Oxygen dynamics near the low waterline during incoming tide. Measurements were made in (A) March and (B) October. (C) Oxygen profiles measured in cores in the laboratory showed no dynamics.

successful. During low tide, oxygen was depleted at the surface, and the sediment was fully anoxic. Although the tide had receded, a thin layer of water still covered the sands. This overlying water layer was aerated, and a steep oxygen gradient existed in the boundary layer, directly adjacent to the sediment surface. On flooding by the incoming tide, a rapid oxygen penetration into the sediment was observed. Within 15 min, oxygen penetrated down to 10 cm or more (i.e., to below the measuring depth of the microsensors; Fig. 5A,B). Sediment cores were brought to the laboratory, and the oxygen profiles were measured within 15 min. Under laboratory conditions, the profiles were highly reproducible on repeated measurement, and oxygen penetrated only 3–5 mm in summer (Fig. 5C) and 6–8 mm in winter (data not shown).

The measurements at the midway line of the sand flat were done with the autonomous profiler, and both O₂ and H₂S were measured simultaneously. Although the dynamics were less pronounced than near the low waterline of the flat, oxygen penetration depths varied considerably. During a measurement series in March 2000, covering a period of 60 h, oxygen was observed down to 9 cm (Fig. 6A), and the average penetration depth was 4–5 cm. These results support the conclusion that the nutrient concentration profiles were affected by advective exchange down to 5 cm depth. The penetration depth of oxygen could be highly variable, increasing from 0 to >8 cm within 1 h and decreasing again to 0 in the next profiling 1 h later. In July 2000, during a similarly long series of measurements of 60 h, oxygen penetration dynamics were less pronounced. Oxygen reached

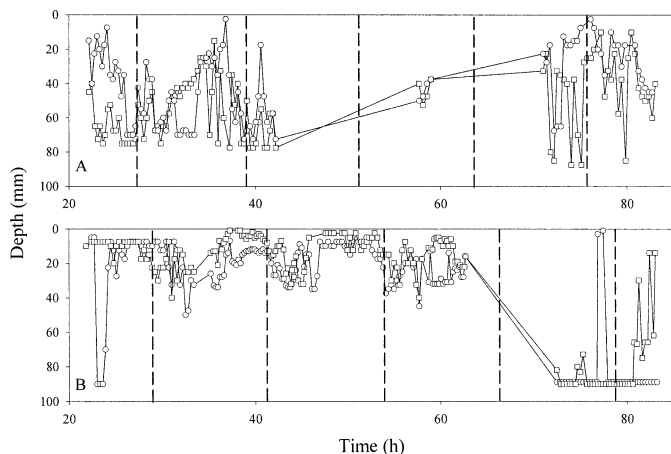


Fig. 6. Oxygen penetration depths measured at the midway line between the high and low waterline. Measurements were made in (A) March and (B) July. The periods without measurement points indicate long service intervals or broken sensors. The last measurement period ($70 < t < 90$ h) in July was strongly influenced by bioturbation. The measurements were made with two oxygen sensors simultaneously; round and square symbols refer to the two different sensors.

depths between 0 and 4 cm (Fig. 6B), averaging 1–2 cm. In this measurement series, the average penetration depth was calculated without the measurements taken on the last day, when the area was subjected to strong bioturbation (as observed from the reworked sediments at the point of micro-sensor penetration), resulting in very deep, irregularly shaped oxygen profiles. A clear response to the incoming tide was not observed in the middle of the sand flat; however, the penetration depth was generally minimal during incoming tide. The penetration depth was the highest during high tide and shortly thereafter, during the falling tide. In July, the two sensors that were deployed ~ 5 cm apart showed similar trends, whereas in March, differences are evident, suggesting more heterogeneous conditions.

Often the profiles were influenced by animal activity, most likely ventilating polychaetes (Fig. 7A). This was apparent from brief oxygen peaks below the sediment surface in deeper zones that were normally anoxic when the sensor crossed horizontal ventilated burrows. These oxygen peaks typically lasted 1 h. When the sensors were placed at or near the vertical shaft of the burrow that extended to the surface, continuous fluctuations were observed during the full 12-h measuring period (Figs. 6B, 7B). The amount of oxygen introduced into the sediments by bioturbation, estimated from the aerated volume and the fraction of the total observation time this volume was present, was $\sim 25\%$ of the total amount of oxygen in the bed.

Photosynthetic activity was apparent from an oxygen peak at 4 mm depth in the sediment during daylight hours. The sensors disturbed the photosynthetic layer during penetration to some extent because the shaft of the sensors increased in diameter with distance from the tip. For accurate determination of maximal net photosynthesis rates, we determined in situ high-spatial resolution profiles on a sunny day in October in very calm weather. There was no wind, and water

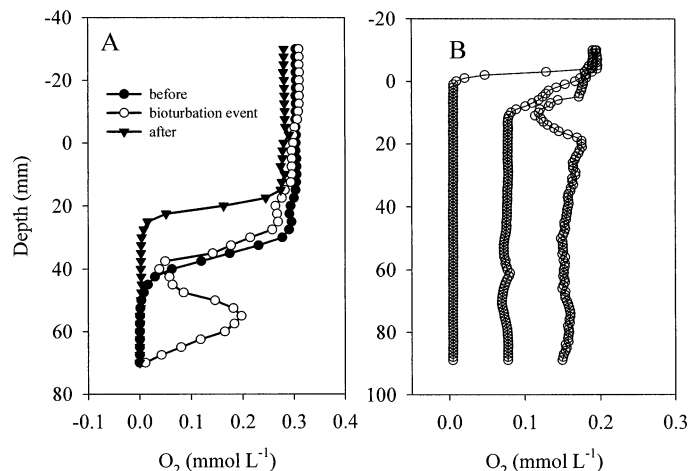


Fig. 7. The effect of bioturbation on in situ oxygen profiles. (A) Shows how profiles are temporarily disturbed by a passing sediment dweller. (B) Shows several profiles measured when the profiler was inadvertently placed above the vertical inlet of an *Arenicola* burrow.

currents over the flat were $< 5 \text{ cm s}^{-1}$, as estimated from particle movement. The measurements were done in the middle of the flat within 30 min after the incoming tide flooded the site. Before each profile measurement, we moved the profiler to a new location. The profiles measured at seven different locations on the flat were remarkably similar (Fig. 8). Assuming diffusion was the dominating transport mechanism at the time of these measurements and a 12-h daily light period, we calculated the oxygen production in the photic zone to be $35 \text{ mmol m}^{-2} \text{ d}^{-1}$. In sediment cores incubated in the laboratory, oxygen profiles were steeper than in the field, with a peak closer to the surface. From these laboratory profiles, a higher productivity in the photic zone was cal-

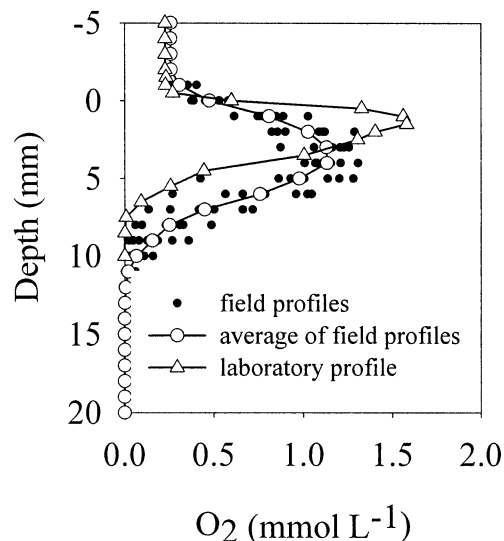


Fig. 8. Oxygen profiles measured during a sunny day in October, showing the effect of photosynthesis. Eight in situ profiles were averaged. Simultaneously, profiles were measured in cores incubated in the laboratory, under ambient temperature and $600 \mu\text{mol photons m}^{-2} \text{ s}^{-1}$.

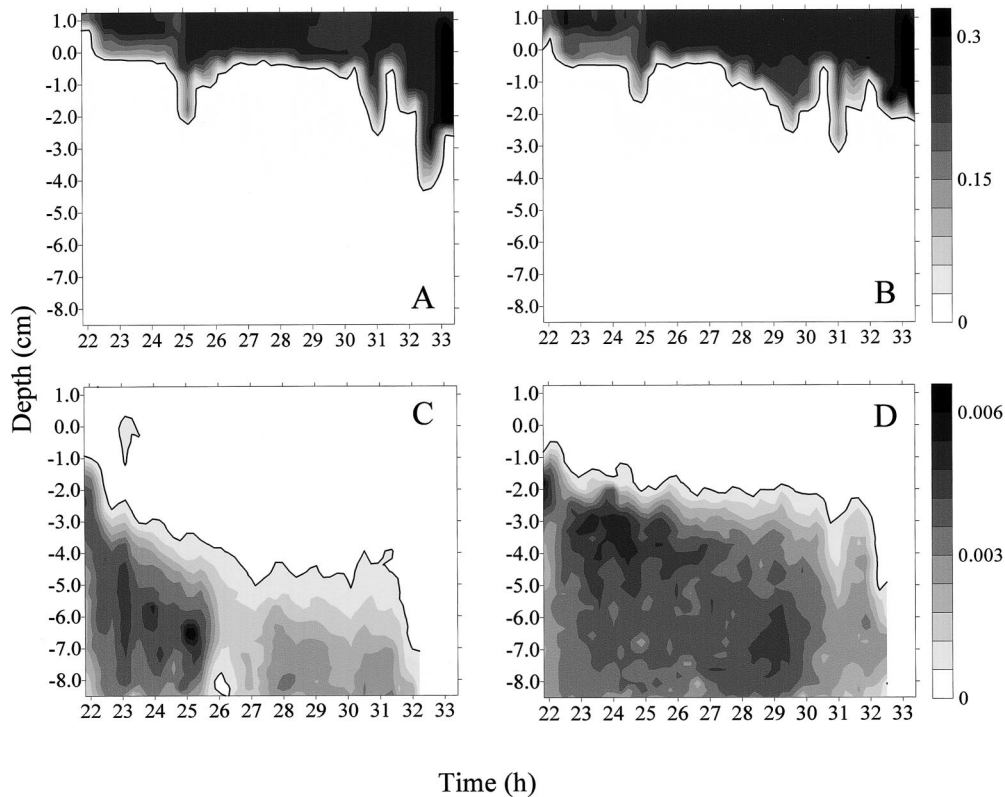


Fig. 9. (A, B) Contour plots of O_2 and (C, D) H_2S during a tidal cycle in July. The single contour line in each plot indicates the detection limit of the sensors (1 mmol m^{-3}). Sulfide and oxygen do not overlap, which is typical for these sediments. The units of the scales on the right are mmol L^{-1} .

culated of $77 \text{ mmol m}^{-2} \text{ d}^{-1}$. The oxygen profiles induced by photosynthesis could be mimicked in the laboratory most closely by a downflow velocity of $1.9 \mu\text{m s}^{-1}$, which corresponds to $160 \text{ L m}^{-2} \text{ d}^{-1}$.

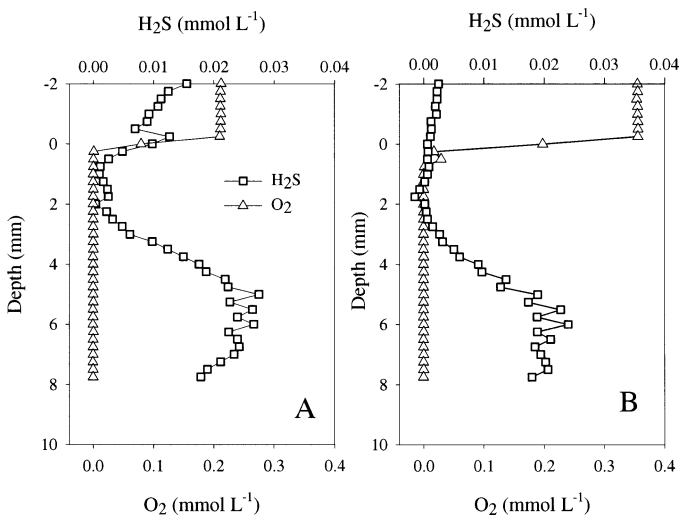


Fig. 10. (A) The only occasion sulfide and oxygen were present simultaneously was when sulfide was found in the water column. (B) This situation lasted several hours until the tide turned and the sulfide concentration in the water column returned to close to 0.

During the in situ measurements, no sulfide was detected during the winter months (March and November), whereas in the summer months (June and September), sulfide was found in the deeper layers, always 2 cm deeper than the lowest oxygen reading (Fig. 9). Both the oxygen penetration depth and the upper sulfide boundary fluctuated, but an overlap was never observed. On one occasion, sulfide was recorded for several hours in the overlying water (Fig. 10A). At the same time, sulfide was measured in the sediments below 2 cm depth, but not in the top 2 cm. Thus, the top 2 cm of the sediment formed a sink for sulfide, although it was anoxic, and aerobic sulfide oxidation can be excluded. The event coincided with unusually low oxygen values. At the turning of the tide, the oxygen values were restored to normal, and sulfide disappeared (Fig. 10B).

Laboratory microsensors studies—To determine whether microsensors profiles measured in the field could be mimicked in the laboratory, we collected several sediment cores and measured oxygen profiles. The in situ measurements showed penetration depths of one order of magnitude larger than those measured in sediment cores taken into the laboratory. To some extent, the measured field profiles could be mimicked experimentally by inducing a vertical water flow through the sediment. One such experiment is shown in Fig. 11A, for which in the absence of vertical flow, oxygen penetrated $\sim 8 \text{ mm}$. On perfusing the cores with seawater in an

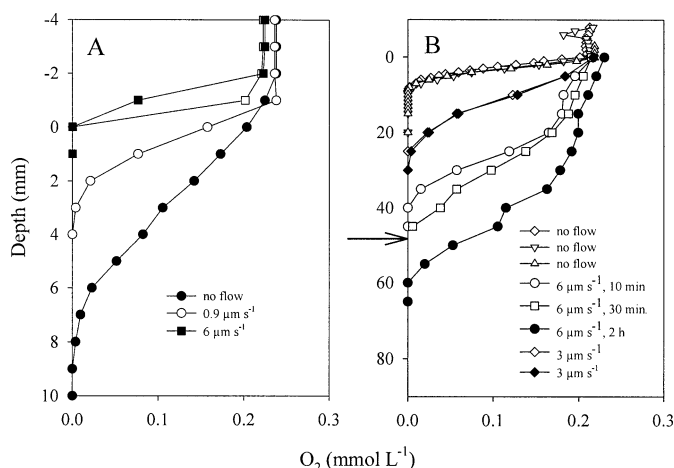


Fig. 11. O_2 profiles measured in the laboratory while imposing vertical flow. (A) When flow is directed upward, oxygen penetration is lower ($0.9 \mu\text{m s}^{-1}$) and becomes 0 at $6 \mu\text{m s}^{-1}$. (B) Shows that downward-directed flow leads to increase of O_2 penetration. The arrow indicates the O_2 penetration depth measured in situ.

upward direction, the penetration depth of oxygen decreased significantly at a flow velocity of $0.9 \mu\text{m s}^{-1}$. At a flow velocity of $6 \mu\text{m s}^{-1}$ and more, the sediments became fully anoxic, as observed in the field at the low waterline during low tide.

On perfusion in a downward direction, the penetration depth of oxygen increased (Fig. 11B). At a flow velocity of $3 \mu\text{m s}^{-1}$, the penetration depth increased from 7 to 20–25 mm, where it remained stable. At a downward flow velocity of $6 \mu\text{m s}^{-1}$, oxygen penetration increased to 40 mm in 10 min, 50 mm in 30 min, and 70–80 mm in 2 h. The oxygen penetration depth in the field averaged ~ 50 mm over a period of 3 d. A flow velocity of $6 \mu\text{m s}^{-1}$ corresponds to a water exchange of $\sim 500 \text{ L m}^{-2} \text{ d}^{-1}$. This amount of seawater exchange agrees with the results of flume experiments on the same sediments for which the effect of waves was quantified (Precht and Huettel 2003). The flow velocities are expressed as piston flow velocities (i.e., not corrected for the sediment porosity of 0.35, which would lead to numbers almost three times higher, to $17 \mu\text{m s}^{-1}$).

Sediment oxygen uptake potential—Potential oxygen consumption rates were determined by perfusing cores with aerated seawater and following the decrease of oxygen over time at a defined position in the sediment after stopping the perfusion. The activity profiles were reproducible within each core, but considerable variation was observed between cores. Therefore, five cores were analyzed per experiment and averaged. The top 2 cm showed the lowest oxygen consumption rates; below 2 cm depth, an increase was observed, with the highest rates at ~ 5 cm, followed by a decrease below 5 cm depth. In March, the volumetric activities of the sediments were about half of those in July (Fig. 12).

The potential activities can be expressed as areal respiration rates by integrating the local activities over the penetration depth. The experimental data were fitted with a third-order polynomial that describes a continuous relation

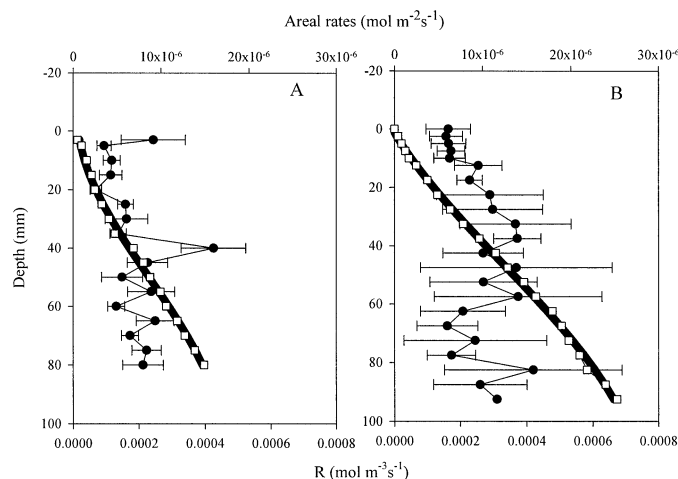


Fig. 12. The local sediment respiration rates, R (closed circles), measured in (A) March and (B) July. From these values, the areal activities were calculated per penetration depth, assuming zero-order kinetics (open squares). The solid line is a fitted third-order polynomial, used to calculate the areal activities from the measured penetration depths.

between penetration depth and areal respiration rates. With the use of this relation, the areal oxygen consumption rates were estimated from the penetration depth of oxygen, as observed by in situ measurements and the sediment activities measured in sediment cores. For simplification, we assumed that oxygen respiration follows zero-order kinetics with respect to oxygen, which means that the local respiration rate is independent of the oxygen concentration. The areal respiration rates calculated over the full observation periods (60–80 h), were $105\text{--}175 \text{ mmol m}^{-2} \text{ d}^{-1}$ both in March and in June. Because the lower volumetric activities in March were compensated with deeper oxygen penetration, the areal rates were equal to those measured in July.

Chamber oxygen consumption rates—At a first glance, the oxygen consumption rates measured in the stirred benthic chambers (49 and $64 \text{ mmol m}^{-2} \text{ d}^{-1}$) were only half the rates calculated from the in situ oxygen penetration and potential local rates. However, the pressure gradients applied in the chambers were relatively low, and the bromide tracer data reveal that the advective pore-water exchange in the chambers ($64 \text{ L m}^{-2} \text{ d}^{-1}$) was lower, by a factor of six to eight, than the flushing rates estimated by the core perfusion technique. Increasing the flow of oxygen-rich water through sandy sediment also increases the consumption rate in permeable sediment; thus, it is not surprising that the chambers predict an oxygen consumption rate that is five times lower than the estimates based on the core perfusion technique.

Sulfate reduction rates—In spite of a high degree of variability for any given sampling period, potential rates of sulfate reduction showed distinct trends consistent with season and temperature. Median sulfate reduction rates during October 1999 and July 2000 were as high as 200 and 99 nmol

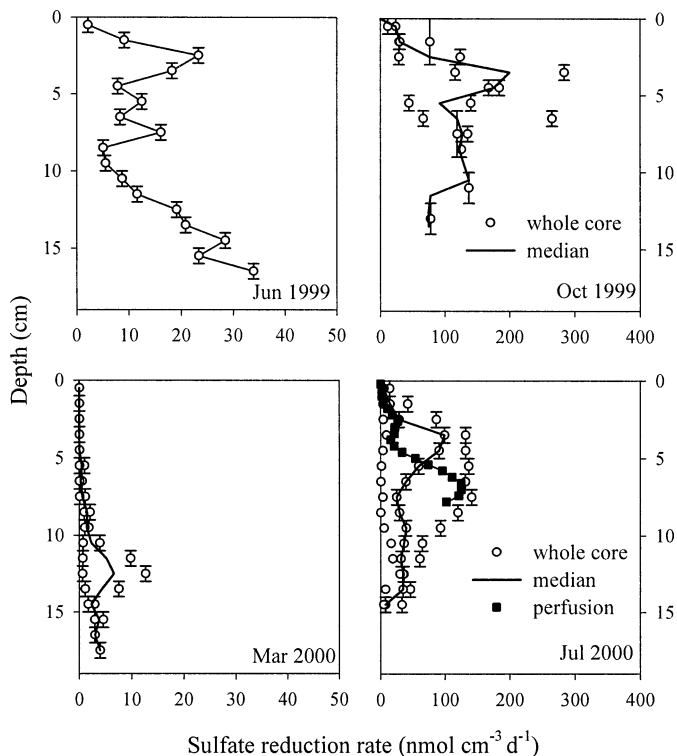


Fig. 13. Profiles of potential sulfate reduction rates versus depth measured at different times of the year by the whole-core method and the perfusion method in July 2000. The median sulfate reduction rate is shown by the solid line.

$\text{cm}^{-3} \text{d}^{-1}$, respectively. Potential sulfate reduction occurred in the surface sediment and increased to peak rates in the 4- to 5-cm layer. Below this peak, rates gradually tapered off to rates of 34 to 78 $\text{nmol cm}^{-3} \text{d}^{-1}$ for July 2000 and October 1999, respectively. Finer scale sampling of sulfate reduction rates in the perfusion core from July 2000 showed that sulfate reduction is only detected below the zone of oxygen penetration (0.4–0.8-cm layer; Fig. 13). (We assume, on the basis of the oxygen penetration experiments for the same core, that oxygen penetration is <4 mm, as shown in Fig. 11.) Sulfate reduction rates in the blackened bands of sediment (4–7 cm) were similar within burrow linings (24–39 $\text{nmol cm}^{-3} \text{d}^{-1}$) and nonburrow-affected sediments (17–35 $\text{nmol cm}^{-3} \text{d}^{-1}$). In the shallower (~ 0 –4 cm) sediments, where rates were distinctly lower than in the black sediments, the burrow linings exhibited enhanced sulfate reduction rates (1.9–13.2 $\text{nmol cm}^{-3} \text{d}^{-1}$) versus nonburrow sediments (0.07–0.47 $\text{nmol cm}^{-3} \text{d}^{-1}$). Integrated rates of sulfate reduction over the upper 15 cm (on the basis of median values) were 2.1 $\text{mmol m}^{-2} \text{d}^{-1}$ in June 1999, 13.7 $\text{mmol m}^{-2} \text{d}^{-1}$ in October 1999, and 7.1 $\text{mmol m}^{-2} \text{d}^{-1}$ in July 2000. In contrast, potential sulfate reduction rates were very low in March 2000. Peak rates were <10 $\text{nmol cm}^{-3} \text{d}^{-1}$ (at a depth of 12–13 cm), and the integrated rate of sulfate reduction >15 cm was a mere 0.08 $\text{mmol m}^{-2} \text{d}^{-1}$. Only below the depth of nitrate penetration (~ 5 cm) was potential sulfate reduction detected in March 2000. The rates of sulfate reduction measured at this site were similar in magnitude and

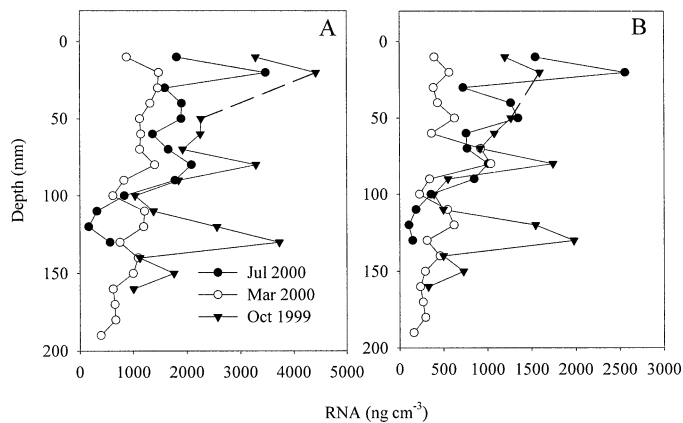


Fig. 14. The distribution of (A) total and (B) bacterial rRNA in October 1999, March 2000, and July 2000.

seasonality to sulfate reduction rates measured in the sandy sediments of nearby Königshafen (Kristensen et al. 2000) and in a sand plate near Westerhever (M. Böttcher pers. comm). They observed that the sulfate reduction rates were strongly temperature dependent (i.e., high rates in summer and low rates in winter).

Total and bacterial RNA content of the sediments—Total rRNA content was determined for three seasons (October 1999, March 2000, and July 2000) by slot blot hybridization (Fig 14). The rRNA concentration based on the universal probe UNI 1390 decreased with depth in all seasons, ranging from 3,473 to 165 ng cm^{-3} sediment in October, from 1,478 to 393 ng cm^{-3} sediment in March, and from 4,419 to 1,006.5 ng cm^{-3} in July. Peaks were observed at 2 cm depth in October at 2, 3, and 8 cm depth in March and at 2, 8, and 13 cm depth in July. The rRNA yields were much lower in March than in October and July, with the highest values obtained in July. The bacterial rRNA, on the basis of the probe EUB 338, followed the same trend as total rRNA, both with depth and over the seasons but with lower values. In October, the bacterial rRNA content varied from 26% to 85%, in March from 26% to 82%, and in July from 29% to 60% of total rRNA.

Organic matter in the water column—Suspended particulate organic carbon (POC) ranged between 20 and 450 $\mu\text{mol C L}^{-1}$. Total POC is not a good measure of readily available organic matter because most of the POC in Wadden Sea suspended matter has a refractory nature (Megens et al. 2001). We estimated the amount of readily available organic matter on the assumption that suspended matter contains two reservoirs of organic matter: a fresh, readily available fraction and a refractory component associated with clay and silt particles. Resuspended sediment (mostly silt and clay) contains mainly refractory carbon, amounting to ~ 3 –4 $\mu\text{mol C mg}^{-1}$ suspended matter, as observed during winter. Fresh, diatom-based organic matter contains ~ 25 $\mu\text{mol C mg}^{-1}$ suspended matter. On the basis of these constants, on the POC content, and on the suspended matter weight, the amount of readily available POC was estimated to be ~ 0 –

10 $\mu\text{mol L}^{-1}$ during winter and $\sim 20\text{--}100 \mu\text{mol L}^{-1}$ during summer. During the spring bloom, fresh POC might shortly increase up to 250 $\mu\text{mol L}^{-1}$ (about 90 μg chlorophyll *a* L^{-1}). Details will be presented elsewhere (van Beusekom pers. comm.).

Discussion

All known measuring equipment will disturb the advective transport within permeable sediments and affect the measured conversion rates. Invasive microsensor techniques, as used in this study, are no exception to this rule. The presence of the sensors is known to induce a reduction in the thickness of the boundary layer (Glud et al. 1994b), whereas the rather large electronic cylinder and the frame to which the electronics and sensors are attached might reduce the current while increasing turbulence. The microsensor approach does have some advantages over traditional chamber methods. With the microprofiler system, the currents are most likely disturbed but certainly not blocked as in chambers. The chambers are either not stirred (D'Andrea et al. 2002) or stirred with a rotating disc (Huettel and Gust 1992; Huettel et al. 1996; Huettel and Rusch 2000), inducing a well-described, but artificial advection pattern (Khalili and Basu 1997). In the latter case, measured conversion rates are influenced by the stirring speed, as indeed was confirmed by our results. A disadvantage of microsensors is that the analysis of bioturbation is strongly biased. It is likely that the presence of moving microsensors induces burrowing organisms to leave the immediate surroundings of the profiler. In chambers, their behavior might be disturbed, but they cannot leave.

No single technique is ideal, and a combination of methods is needed to obtain as precise as possible an estimate of the activity of porous sand. We also need to search for alternative techniques with a minimal effect on the advective flow patterns. A highly promising option is the use of the eddy correlation technique (Berg et al. 2003). This technique measures the total oxygen uptake rates of sediments plus infauna noninvasively from an area upstream of the area under investigation. It determines vertical flux from the difference between downward and upward oxygen transport. The technique was not yet available at the time of our studies. A combination of invasive microsensor measurements, chamber deployments, and the eddy correlation technique might give the best available combination of mechanistic insights and real exchange rates.

Despite the limitations of the techniques used in this study, conclusions can be drawn from our data. The microsensor data show that the sediment–water exchange, as well as the transport of oxygen in the upper 5–10 cm, is dominated by advection, whereas diffusion is insignificant by comparison. The actual oxygen penetration depths, as measured in the field, are always much higher than in diffusion-controlled laboratory measurements. Several driving forces for the observed advection will be discussed: (1) tides, (2) currents and waves, and (3) burrowing animals.

Tides—The dynamics of oxygen penetration strongly suggest a draining of the sand flat at low tide, resulting in the

outflow of anoxic pore water at the low waterline. Oxygen could not penetrate into the sediment when the flat was dry, although one would expect that close contact with the atmosphere would facilitate oxygen influx. Only with the incoming tide was oxygen able to penetrate into the sediment, sometimes at very high rates. The data are consistent with a model analogous to communicating vessels, in which a water reservoir below the sand flat or the island is in horizontal exchange with the seawater. However, this model only partly explains the observed phenomena. Surprisingly, a rather low pressure difference, induced by a few centimeters of water during the incoming tide, was sufficient to reverse outflow to inflow. This indicates that the exchanging reservoir is close to the low waterline, otherwise the resistance to water flow in the sediment would be too high to induce such a rapid and strong response. The outflow is not compensated for by inflow at the midway waterline of the flat. We did not observe air entering the pore space, and the surface always remained water saturated. Possibly, the sediments expand on inundation and shrink during low tide (e.g., by tide-regulated activity of sediment-dwelling organisms or by physical forces; T. Shaw pers. comm.). If this is the case, the inflow could be a short-time event, directly following the incoming tide, and quantitatively not very significant for the exchange of seawater and pore water. Further measurements with the autonomous profiler are needed to clarify this issue.

Currents and waves—At the midway line of the sand flat, no striking influx of oxygen with the incoming tide was observed. Here, the dynamics were caused by the action of currents and waves. Currents induce interfacial exchange as a result of small pressure differences over ripples, leading to pore-water outflow near the top of a ripple and inflow at the base. Continuously moving ripples and currents that are irregular in velocity and direction will induce a constantly changing mosaic of inflow and outflow at the sediment surface. Waves will contribute to the pattern of advective cells at the seafloor, when the wave height is at least half the water depth (Precht and Huettel 2003). Although the site is rather protected, currents of up to 40 cm s^{-1} and waves of up to 1 m were observed. These dynamics could well explain the irregular oxygen penetration pattern as seen from the profiler data.

The average penetration of oxygen, measured over several days, can be mimicked in the laboratory by inducing a downward perfusion of the sediment with aerated seawater. From these comparisons, we concluded that 160–500 $\text{L m}^{-2} \text{d}^{-1}$ can be exchanged (i.e., 16–50 cm of the overlying water column). Of course, the advective mechanism is not perfectly mimicked because the natural alternating flow regime, with decreasing flow rates with depth, was mimicked by a unidirectional flow that was constant with depth. Because oxygen penetration is more effectively stimulated under laboratory conditions, we have probably underestimated the volumetric exchange rate. Because the Wadden Sea is, on average, 1.5 m deep and 70% of the sediments are sandy, the entire waterbody can pass through the sandy sediment within 3–10 d. This should have a strong effect on seawater chemistry and the degradation of suspended organic matter.

Burrowing animals—Finally, we have observed activities of burrowing animals that can strongly influence water exchange. Our measuring strategies were not ideal for quantifying this effect, and the equipment used might have disturbed the macrofauna. Certainly the degradation of organic carbon is enhanced in burrows and burrow linings, as demonstrated by the increased sulfate reduction rates in burrow linings. The effect of burrowing on the exchange rates has been discussed extensively in many publications (e.g., Kristensen 2000; Felder 2001; Reise 2002). Taken together, there is good evidence that the presence of burrowing organisms might significantly add to the exchange of seawater with the sediment.

Annual primary production in the North Frisian Wadden Sea amounts to 25 mol C m^{-2} (303 g C m^{-2}). Pelagic and benthic primary production contribute in equal amounts, whereas sea grass production is negligible (Asmus et al. 1998). Total annual remineralization in the North Frisian Wadden Sea amounts to about 33 mol C m^{-2} (400 g C m^{-2}), with the water column and benthic processes contributing similar amounts (Van Beusekom et al. 1999). The difference between total production and remineralization of about 8 mol C m^{-2} (100 g C m^{-2}) is in line with the heterotrophic nature of the Wadden Sea (Postma 1954; Van Beusekom et al. 1999). The estimates of benthic mineralization were mainly based on core and chamber incubations and therefore might have underestimated the benthic mineralization rates by excluding advective processes.

The oxygen consumption rate calculated from our data was on the order of $140 \text{ mmol m}^{-2} \text{ d}^{-1}$ in March and June. For this oxygen consumption, a stoichiometric amount of an electron donor is needed. This can originate from in situ benthic photosynthesis, from land through the aquifer or by wind, or from POC filtered from seawater. Under ideal conditions on a sunny day in October, O_2 production from photosynthesis was $35 \text{ mmol m}^{-2} \text{ d}^{-1}$; on a yearly average, the production is presumably much lower. Terrestrial input could not be determined in this study. The contribution of an electron donor from seawater can be calculated from the concentration of organic material and the amount of seawater exchange, assuming that the sediments are a perfect trap for the organic material. Suspended POC ranged between 20 and $450 \text{ mmol C m}^{-3}$. However, most of the organic matter associated with Wadden Sea suspended matter is of refractory nature (Megens et al. 2001). It was estimated that, in the North Frisian Wadden Sea, about 20% of the POC is associated with phytoplankton biomass. Therefore, total POC is not a good measure of readily available organic matter. We estimated the concentration of fresh organic matter in the water column on the basis of the assumption that suspended matter contains two types of organic matter: a fresh, readily available fraction and a refractory fraction associated with clay and silt particles. The degradable POC in the seawater overlying the sediment varied strongly with the season. The degradable C (org-C) content was estimated to be 8 mmol m^{-3} in January–February 2001; $60 \text{ mmol org-C m}^{-3}$ in early spring 2001, with peaks up to $250 \text{ mmol org-C m}^{-3}$; $50 \text{ mmol org-C m}^{-3}$ in May–July; $25 \text{ mmol org-C m}^{-3}$ in August–September; and $13 \text{ mmol org-C m}^{-3}$ in October–De-

cember 2001. The weighted average over a year was 33 mmol m^{-3} ; the mean summer value was 45 mmol m^{-3} . It should be emphasized that this calculation results in a highly conservative estimate of the amount of degradable organic matter. The average amount of degradable POC ($\sim 35 \text{ mmol m}^{-3}$), together with seawater exchange with the sediment ($0.5 \text{ m}^3 \text{ m}^{-2}$) would lead to an organic C input of $17 \text{ mmol m}^{-2} \text{ d}^{-1}$ when averaged over a year. The spring bloom would have resulted in an input of $\sim 30 \text{ mmol m}^{-2} \text{ d}^{-1}$ in the March period, and during the peak, $125 \text{ mmol m}^{-2} \text{ d}^{-1}$. In June, the calculated C input would have been $\sim 25 \text{ mmol m}^{-2} \text{ d}^{-1}$. The sum of the benthic production ($35 \text{ mmol org-C m}^{-2} \text{ d}^{-1}$) plus the estimated input from seawater POC ($17 \text{ mmol org-C m}^{-2} \text{ d}^{-1}$) does not balance the calculated oxygen consumption rate ($105\text{--}175 \text{ mmol org-C m}^{-2} \text{ d}^{-1}$).

One explanation for the discrepancy between the electron donor and acceptor input estimated here is that the actual carbon fluxes have been higher or the concentration of electron donor in the seawater is underestimated. Our estimation of the degradable portion of POC certainly is conservative, and the actual amount of degradable POC input will be higher. Part of what we have labeled as refractory input will be bioavailable, although its degradation is at a lower rate. Moreover, the near-bed transport of organic material was not determined accurately. Our data are based on surface water samples, whereas bottom-water sampling would have led to better approximations of the POC input into the sediments. Furthermore, the site is not typical for the Wadden Sea because the sand plate is situated near the coast. Thus, floating organic material accumulates on the beach, is macerated in the coarse sand by the action of waves, and is made readily available for degradation inside the sands. The organic input in the middle of the Wadden Sea might be lower. A point of uncertainty is the role of dissolved organic carbon (DOC). No data on DOC in the northern Wadden Sea are available, and it is not clear yet whether Wadden Sea sediments act as a sink or as a source of DOC. Some indications of the bioavailable DOC can be derived from recently dissolved organic phosphorus measurements that show a distinct seasonal cycle with low concentrations of about $0.15 \mu\text{mol L}^{-1}$ during winter and a maximum of about $0.8 \mu\text{mol L}^{-1}$ during summer. Assuming that a Redfield ratio in fresh DOC yields available DOC concentrations of $15\text{--}80 \mu\text{mol L}^{-1}$, advection of DOC into and mineralization of DOC within the sediment might therefore double the total amount of O_2 consumption in the sediment. Further research is needed to quantify the role of Wadden Sea sediments as a sink or source of DOC.

Reduced compounds derived from the reduction of other terminal electron acceptors (e.g., MnO_2 , oxidized iron, or sulfate) might also contribute substantially to oxygen consumption in well-irrigated sediments. Sulfate reduction rates in sandy sediments studied here are comparable to the nearby sandy sediments of Königshafen (Kristensen et al. 2000). They are also comparable to other nearshore muddy sites (e.g., Aarhus Bay; Thamdrup et al. 1994) where sulfate reduction accounts for nearly one half of all the oxygen uptake (Jørgensen 1996). However, the relative importance of sulfate reduction for organic carbon mineralization in the Sylt sediments is reduced by the high input of oxygen. As a result, the oxygen consumption rates are at least 20-fold higher

than integrated sulfate reduction rates. Therefore, the oxidation of reduced substances, such as sulfide, Fe(II), or Mn(II), must only play a minor role in oxygen consumption.

Nevertheless, active sulfur cycling is occurring in these sediments that is more dynamic than in muddy sediments. Our measurements show that sulfide was both produced and consumed or continuously bound in the top 5 cm of the sediment, indicating that a pool of oxidizing power other than oxygen resided in the top layer of the sediments. On the basis of the potential sulfate reduction rates, turnover times of sulfide within this zone are on the order of hours to minutes, whereas deeper in the sediment (i.e., below 5 cm), turnover times are days to weeks. As discussed by Zopfi et al. (2001 and references therein), biological sulfide oxidation is independent of sulfide or oxygen concentrations over a wide range of substrate concentrations. Furthermore, the K_m values of sulfide-oxidizing organisms are such that sulfide can be oxidized rapidly to submicromolar concentrations.

Interestingly, free sulfide and oxygen did not overlap in the sediment. This means that the sulfide produced by sulfate reduction is oxidized anaerobically. The possible electron acceptors for sulfide oxidation are oxidized iron and nitrate. We hypothesize that the relatively large pool of Fe(III) oxyhydroxide ($\sim 1 \mu\text{mol cm}^{-3}$ in the upper 10 cm of sediment) provides the oxidizing reservoir needed to scavenge and oxidize H_2S . FeS is temporarily formed on reaction of Fe(II) with an excess of H_2S . On increased O_2 penetration, FeS is reoxidized by O_2 to Fe(III)OOH, elemental sulfur, polythionates, thiosulfate, and ultimately sulfate (von Rége 1999). Contents of both Fe(III) and Mn(IV) in the sediments do not reach levels in which a significant contribution of bacterial heterotrophic metal oxide reduction is expected (Thamdrup 2000). Only a small percentage of the total oxygen demand is required to flush and oxidize the sediment on a regular basis, so as to maintain this high level of oxidizing capacity. This is analogous to the reoxidation of muddy, but permeable (because of high polychaete populations), shelf sediments off central Chile (Ferdelman et al. 1997). Nitrate was found in the pore water in March 2000, and on several occasions we found *Beggiatoa*, large sulfur-oxidizing gliding bacteria, that can store nitrate (Schulz and Jørgensen 2001). These organisms separate sulfide and oxygen profiles effectively by oxidizing sulfide with stored nitrate. At our field site, these bacteria appeared to be rare and occurred in patches. Therefore, they are unlikely to play a significant role in sulfide oxidation. The presence of sulfide in the overlying water on one occasion cannot be explained fully. The sulfide could have leaked out of the sediment or originated from floating, decaying biomass. The kinetics of chemical sulfide oxidation is quite sluggish compared to biological sulfide oxidation (Zopfi et al. 2001).

Ribosomal RNA quantification can yield information about microbial activity. The decrease in total and bacterial rRNA concentrations with depth in all three cores indicates that microbial activity is higher in the upper sediment layers in which the input of organic material from the water column occurs. Also, the seasonal trends in RNA patterns correspond with the rate measurements. Sulfate reduction and volumet-

ric aerobic respiration rates were much lower in March than in July.

The degradation potential and organic conversion rates in porous sands seem to be high, mainly because of the efficient input of oxygen and organic matter. The large advective stimulation of the aerobic degradation clearly points to the need for in situ monitoring to appreciate the importance of porous sandy sediments. This high throughput of oxygen also maintains low sulfide concentrations in the surface 5 cm, in spite of active sulfate reduction activity throughout the sandy sediments. Although sulfur cycling is highly active, the comparison of intertidal sand flats with aerobic sand filters (D'Andrea et al. 2002) appears to be well chosen.

References

- AMANN, R. I., B. J. BINDER, R. J. OLSON, S. W. CHISHOLM, R. DEVEREUX, AND D. A. STAHL. 1990. Combination of 16S rRNA-targeted oligonucleotide probes with flow cytometry for analyzing mixed microbial populations. *Appl. Environ. Microbiol.* **56**: 1919–1925.
- ARCHER, D., S. EMERSON, AND C. REIMERS. 1989. Dissolution of calcite in deep-sea sediments: pH and O_2 microelectrode results. *Geochim. Cosmochim. Acta* **53**: 2831–2845.
- ASMUS, R., M. H. JENSEN, D. MURPHY, AND R. DOERFFER. 1998. Primärproduktion von Mikrophytobenthos, Phytoplankton und jährlicher Biomassertrag des Makrophytobenthos im Sylt-Rømø Wattenmeer, p. 367–392. *In* C. Gätje and K. Reise [eds.], *Ökosystem Wattenmeer: Austausch, Transport und Stoffwandlungsprozesse*. Springer Verlag.
- BERG, P., N. RISGAARD-PEDERSEN, AND S. RYSGAARD. 1998. Interpretation of measured concentration profiles in sediment pore water. *Limnol. Oceanogr.* **43**: 1500–1510.
- , H. RØY, F. JANSSEN, V. MEYER, B. B. JØRGENSEN, M. HUETTEL, AND D. DE BEER. 2003. Oxygen uptake by aquatic sediments measured with a novel non-invasive eddy correlation technique. *Mar. Ecol. Prog. Ser.* **261**: 75–83.
- BOOIJ, K., W. HELDER, AND B. SUNDBY. 1991. Rapid redistribution of oxygen in a sandy sediment induced by changes in the flow velocity of the overlying water. *Neth. J. Sea. Res.* **28**: 149–165.
- CANFIELD, D. E. 1989. Reactive iron in marine sediments. *Geochim. Cosmochim. Acta* **53**: 619–632.
- D'ANDREA, A. F., R. C. ALLER, AND G. R. LOPEZ. 2002. Organic matter flux and reactivity on a South Carolina sandflat: The impacts of porewater advection and macrobiological structures. *Limnol. Oceanogr.* **47**: 1056–1070.
- FELDER, D. 2001. Diversity and ecological significance of deep-burrowing macrocrustaceans in coastal tropical waters of the Americas (Decapoda: Thalassinidea). *Interciencia* **26**: 440–449.
- FERDELMAN, T. G., C. LEE, S. PANTOJA, J. HARDER, B. BEBOUT, AND H. FOSSING. 1997. Sulfate reduction and methanogenesis in a *Thioploca*-dominated sediment off the coast of Chile. *Geochim. Cosmochim. Acta* **61**: 3065–3079.
- FORSTER, S., M. HUETTEL, AND W. ZIEBIS. 1996. Impact of boundary layer flow velocity on oxygen utilisation in coastal sediments. *Mar. Ecol. Prog. Ser.* **143**: 173–185.
- FOSSING, H., AND B. B. JØRGENSEN. 1989. Measurement of bacterial sulfate reduction in sediments: Evaluation of single-step chromium reduction method. *Biogeochemistry* **8**: 205–222.
- GLUD, R. N., J. K. GUNDERSEN, B. B. JØRGENSEN, N. P. REVSBECH, AND H. D. SCHULZ. 1994a. Diffusive and total oxygen uptake of deep-sea sediments in the eastern South Atlantic Ocean: In

- situ and laboratory measurements. *Deep-Sea Res. I* **41**: 1767–1788.
- GLUD, R. N., J. K. GUNDERSEN, N. P. REVSBECH, AND B. B. JØRGENSEN. 1994b. Effects on the benthic diffusive boundary layer imposed by microelectrodes. *Limnol. Oceanogr.* **39**: 462–467.
- GRASSHOFF, K., K. KREMLING, AND M. EHRHARDT. 1999. *Methods of seawater analysis*. Wiley.
- GUNDERSEN, J. K., AND B. B. JØRGENSEN. 1990. Microstructure of diffusive boundary layers and the oxygen uptake of the sea floor. *Nature* **345**: 604–607.
- HUETTEL, M. 1990. Influence of the lugworm *Arenicola marina* on porewater nutrient profiles of sand flat sediments. *Mar. Ecol. Prog. Ser.* **62**: 241–248.
- , AND G. GUST. 1992. Solute release mechanisms from confined sediment cores in stirred benthic chambers and flume flows. *Mar. Ecol. Prog. Ser.* **82**: 187–197.
- , AND A. RUSCH. 2000. Transport and degradation of phytoplankton in permeable sediments. *Limnol. Oceanogr.* **45**: 534–549.
- , W. ZIEBIS, AND S. FORSTER. 1996. Flow-induced uptake of particulate matter in permeable sediments. *Limnol. Oceanogr.* **41**: 309–322.
- JEROSCHEWSKI, P., C. STEUKART, AND M. KÜHL. 1996. An amperometric microsensor for the determination of H₂S in aquatic environments. *Anal. Chem.* **68**: 4351–4357.
- JICKELLS, T. D., AND J. E. RAE. 1997. Biogeochemistry of intertidal sediments, p. 1–15. *In* T. D. Jickells and J. E. Rae [eds.], *Biogeochemistry of intertidal sediments*. Cambridge Univ. Press.
- JØRGENSEN, B. B. 1978. A comparison of methods for the quantification of bacterial sulfate reduction in coastal marine sediments. I. Measurement with radiotracer techniques. *Geomicrobiol. J.* **1**: 29–47.
- . 1996. Case study—Aarhus Bay, p. 137–154. *In* B. B. Jørgensen and K. Richardson [eds.], *Eutrophication in coastal marine ecosystems*. Coastal and estuarine studies. American Geophysical Union.
- KEIL, R., D. MARTLUCAN, F. PRAHL, AND J. HEDGES. 1994. Sorptive preservation of labile organic matter in marine sediments. *Nature* **370**: 549–552.
- KERNER, M. 1993. Coupling of microbial fermentation and respiration processes in an intertidal mudflat of the Elbe estuary. *Limnol. Oceanogr.* **38**: 314–330.
- , AND S. YASSERI. 1997. Utilization of phytoplankton in seston aggregates from the Elbe estuary, Germany, during early degradation processes. *Mar. Ecol. Prog. Ser.* **158**: 87–102.
- KHALILI, A., AND A. J. BASU. 1997. A non-Darcy model for recirculating flow through a fluid–sediment interface in a cylindrical container. *Acta Mech.* **123**: 75–87.
- KLUTE, A., AND C. DIRKSEN. 1986. Hydraulic conductivity and diffusivity: Laboratory methods, p. 687–700. *In* A. Klute [ed.], *Methods of soil analysis—part 1—physical and mineralogical methods*. American Society of Agronomy.
- KOMADA, T., C. E. REIMERS, AND S. E. BOEHME. 1998. Dissolved inorganic carbon profiles and fluxes determined using pH and pCO₂ microelectrodes. *Limnol. Oceanogr.* **43**: 769–781.
- KRISTENSEN, E. 2000. Organic matter diagenesis at the oxic/anoxic interface in coastal marine sediments, with emphasis on the role of burrowing animals. *Hydrobiologia* **426**: 1–24.
- , H. BODENBENDER, M. H. JENSEN, H. RENNENBERG, AND K. M. JENSEN. 2000. Sulfur cycling of intertidal Wadden Sea sediments (Königshafen, Island of Sylt, Germany): Sulfate reduction and sulfur gas emission. *J. Sea Res.* **43**: 93–104.
- LLOBET-BROSSA, E., AND OTHERS. 2002. Community structure and activity of sulfate reducing bacteria in an intertidal surface sediment: A multi-method approach. *Aquat. Microb. Ecol.* **29**: 211–226.
- LLOBET-BROSSA, E., R. ROSSELLO-MORA, AND R. AMANN. 1998. Microbial community composition of Waddensea sediments as revealed by fluorescence in situ hybridisation. *Appl. Environ. Microbiol.* **64**: 2691–2696.
- MACGREGOR, B. J., D. P. MOSER, E. W. ALM, K. H. NEALSON, AND D. A. STAHL. 1997. Crenarchaeota in Lake Michigan sediment. *Appl. Environ. Microbiol.* **63**: 1178–1181.
- MALCOLM, S. J., AND D. B. SIVYER. 1997. Nutrient recycling in intertidal sediments, p. 59–99. *In* T. D. Jickells and J. E. Rae [eds.], *Biogeochemistry of intertidal sediments*. Cambridge Univ. Press.
- MARTENS, P., AND M. ELBRÄCHTER. 1998. Zeitliche und räumliche Variabilität der Mikronährstoffe und des Planktons im Sylt Römø Wattenmeer, p. 65–79. *In* C. Gätje and K. Reise [eds.], *Ökosystem Wattenmeer*. Springer.
- MEGENS, L., J. VAN DER PLICHT, AND J. W. DE LEEUW. 2001. Temporal variations in C-13 and C-14 concentrations in particulate organic matter from the southern North Sea. *Geochim. Cosmochim. Acta* **65**: 2899–2911.
- POSTMA, H. 1954. Hydrography of the Dutch Wadden Sea. *Arch. neerl. Zool.* **10**: 405–511.
- PRECHT, E., AND M. HUETTEL. 2003. Advective pore water exchange driven by surface gravity waves and its ecological implications. *Limnol. Oceanogr.* **48**: 1674–1684.
- REISE, K. 2002. Sediment mediated species interactions in coastal waters. *J. Sea Res.* **48**: 127–141.
- REVSBECH, N. P. 1989. An oxygen microelectrode with a guard cathode. *Limnol. Oceanogr.* **34**: 474–478.
- ROCHA, C., AND A. P. CABRAL. 1998. The influence of tidal action on porewater nitrate concentration and dynamics in intertidal sediments of the Sado estuary. *Estuaries* **21**: 635–645.
- RUSCH, A., AND M. HUETTEL. 2000. Advective particle transport into permeable sediments—evidence from experiments in an intertidal sandflat. *Limnol. Oceanogr.* **45**: 525–533.
- RUTGERS VAN DER LOEFF, M. M. 1981. Wave effects on sediment water exchange in a submerged sand bed. *Neth. J. Sea Res.* **15**: 100–112.
- SCHULZ, H. N., AND B. B. JØRGENSEN. 2001. Big bacteria. *Ann. Rev. Microbiol.* **55**: 105–137.
- SHUM, K. T., AND B. SUNDBY. 1996. Organic matter processing in continental shelf sediments—the subtidal pump revisited. *Mar. Chem.* **53**: 81–87.
- STAHL, D. A., B. FLESHER, H. R. MANSFIELD, AND L. MONTGOMERY. 1988. Use of phylogenetically based hybridization probes for studies of ruminal microbial ecology. *Appl. Environ. Microbiol.* **54**: 1079–1084.
- THAMDRUP, B. 2000. Bacterial manganese and iron reduction in aquatic sediments. *Adv. Microbiol. Ecol.* **16**: 41–84.
- , H. FOSSING, AND B. B. JØRGENSEN. 1994. Manganese, iron, and sulfur cycling in a coastal marine sediment, Aarhus Bay, Denmark. *Geochim. Cosmochim. Acta* **58**: 5115–5129.
- VAN BEUSEKOM, J. E. E., U. H. BROCKMANN, K. J. HESSE, W. HICKEL, K. POREMA, AND U. TILLMANN. 1999. The importance of sediments in the transformation and turnover of nutrients and organic matter in the Waddensea and German Bight. *Dtsche Hydrogr. Z.* **51**: 245–266.
- VON RÉGE, H. 1999. Bedeutung von Mikroorganismen des Schwefelkreislaufes für die Korrosion von Metallen. *Univ. of Hamburg*.
- WENZHÖFER, F., AND R. N. GLUD. 2002. Benthic carbon mineralization in the Atlantic: A synthesis based on in situ data from the last decade. *Deep-Sea Res. I* **49**: 1255–1279.
- , O. HOLBY, R. N. GLUD, H. K. NIELSON, AND J. K. GUN-

- DERSEN. 2000. In situ microsensor studies of a shallow water hydrothermal vent at Milos, Greece. *Mar. Chem.* **69**: 43–45.
- ZHENG, D., E. W. ALM, D. A. STAHL, AND L. RASKIN. 1996. Characterization of universal small subunit rRNA hybridization probes for quantitative molecular microbial ecology studies. *Appl. Environ. Microbiol.* **62**: 4504–4513.
- ZIEBIS, W., M. HUETTEL, AND S. FORSTER. 1996. Impact of biogenic sediment topography on oxygen fluxes in permeable seabeds. *Mar. Ecol. Prog. Ser.* **140**: 227–237.
- ZOPFI, J., T. G. FERDELMAN, B. B. JØRGENSEN, A. TESKE, AND B. THAMDRUP. 2001. Influence of water column dynamics on sulfide oxidation and other major biogeochemical processes in the chemocline of Mariager Fjord (Denmark). *Mar. Chem.* **74**: 29–51.

Received: 2 March 2004

Accepted: 24 June 2004

Amended: 26 July 2004